The College of Engineering
University of Wisconsin-Madison

Wisconsin Electric Machines and Power Electronics Consortium

RESEARCH REPORT
87-21

Simulation of a Four Phase Switched Reluctance Motor Including the Effects of Mutual Coupling

Thomas A. Lipo and Julio C. Moreira
Department of Electrical and Computer Engineering
University of Wisconsin
Madison, Wisconsin 53713, U.S.A.

WEMPEC

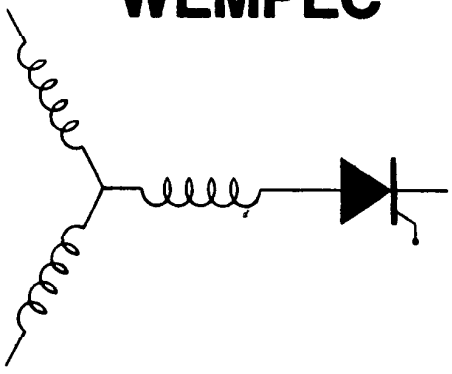

Department of Electrical and Computer Engineering
1415 Johnson Drive
Madison, Wisconsin 53706

June 1987

SIMULATION OF A FOUR PHASE SWITCHED RELUCTANCE MOTOR INCLUDING THE EFFECTS OF MUTUAL COUPLING

Thomas A. Lipo and Julio C. Moreira
Department of Electrical and Computer Engineering
University of Wisconsin
Madison, Wisconsin 53706, U.S.A.

Abstract

Switched reluctance motors are typically constructed such that the coupling between phases is relatively small compared to conventional induction and synchronous machines. While small, this coupling is not negligible and could have important influence on transfer of current between motor phases during both normal and abnormal conditions. This paper presents, for the first time, a coupled circuit model which allows for mutual coupling between motor phases. Comparison is made between simulation and test results and good correlation is obtained.

1 INTRODUCTION

During recent years, interest in has been growing in the use of switched reluctance motors for variable speed drive applications. Because of its simple and rugged construction together with its low cost, the motor is being considered for drive applications ranging from fractional horsepower drives for home appliances to high horsepower traction drives [1,2]. Initial experience indicates that system efficiencies somewhat in excess of conventional PWM adjustable speed induction motor drives are possible over a wide speed range [3].

The switched reluctance (SR) motor is, in effect, a traditional stepping motor which has been optimized to maximize its average torque per rms ampere which is achieved by careful control of the winding currents as a function of shaft position. Hence, feedback control is generally necessary whereas the conventional stepper motor is typically operated open loop. SR motors are almost invariably equipped with an even number of stator and rotor poles. Motor excitation is supplied to concentrated windings on the stator poles while the rotor is a simple laminated structure without windings. The stator poles are excited in pairs when two of the rotor poles approach the stator pole pair and a torque is created which tends to align the poles. The current is rapidly removed when alignment is nearly achieved. Other pairs of stator poles are similarly energized so that the torque developed pulsates but with an average value resulting in continuous rotation of the rotor. The synchronization of the switch- on of the stator excitation is readily accomplished with rotor position feedback.

As present, research on the SR machine has centered primarily on prediction of steady-state behavior since the design of this machine has been of primarily interest [1,4,5]. Steady-state behavior has also been important in the formulation of control strategies [6]. However, impending applications of SR motors in significant horsepower levels will require a thorough analysis of transient behavior as well as steady-state behavior since many normal as well as failure modes require such an analysis.

Thus far, simulation of SR motor drives is in its infancy. Typical of the simulations which have appeared is the work of Stephenson and Corda [7]. In this paper it is assumed that the SR motor is controlled such that current flows in only one of the stator windings at any instant. Since the rotor is not equipped with windings and induced currents in the laminated are neglected, solution of the transient behavior of the motor reduces to the solution of a single non-linear first order differential equation. The computer is programmed so that as the motor rotates, the state-equation of the SR motor remains first order for all winding connections. Hence, it is only necessary to continuously solve only a first order equation for the motor current for all time instants and to simply assign the current being solved to phases $a, b, c, ..$ etc. as the motor rotates.

In Ref. 7 and in others [8,9] it is assumed that since the poles are located along the air gap in diametrically opposite pairs, the MMF drop in the iron is symmetrical over both halves of the stator iron so that the mutual coupling between phases is negligible. Hence, the motor currents in each phase can be calculated as if currents in the remaining phases did not exist. In practice, however, coupling does exist between the motor phases. This coupling is easily verified by exciting one of the motor phases with an *ac* voltage and observing the voltage on the terminals of the remaining open-circuited phases. In addition, presence of RC switching aids (snubbers) combine with the winding inductances to produce oscillatory currents and flux linkages in all phases of the machine after each switching instant. Since the snubbers form ohmic connections between windings, currents in the motor phases cannot be calculated independently.

A complete model of the motor is also necessary for the analysis of unbalanced and faulted modes of operation. In many cases such modes are of great importance since the rating of switches, temperature rise in the machine, magnitude of pulsating torques etc. are often limited by such conditions. Both normal and abnormal modes typically involve conditions under which two or more phases conduct simultaneously. Coupling between phases could clearly have an important influence on the behavior of the drive and a simple uncoupled first order solution is inadequate. This paper presents a new analytical model for the simulation of a switched reluctance motor drive. The analysis specifically concerns the simulation of the popular 8 stator pole/6 rotor pole configuration but can be readily extended to any numbers of stator and rotor poles. The simulation is verified by correlation with actual test results.

2 PRINCIPLE OF OPERATION

Figure 1 shows a pictorial representation of the 8/6 pole SR machine under consideration. This machine is probably the most popular of the switched reluctance motor family since the number of

switches are minimized if a center-tapped dc link is utilized. Also, since the motor rotates in 15 degree steps, torque pulsations are relatively small. Hence, the configuration is favored for battery-vehicle and industrial applications [3].

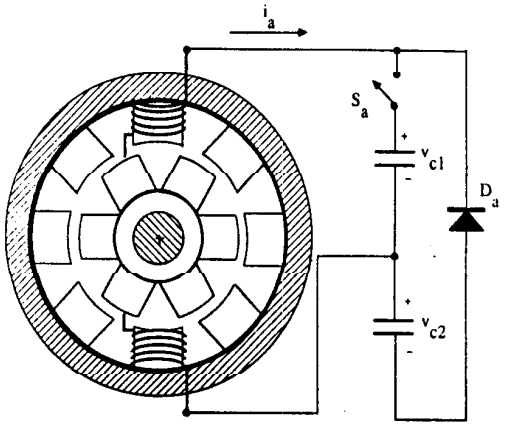

Figure 1: 8 Pole Stator / 6 Pole Rotor Switched Reluctance Motor Showing Idealized Winding for One Phase Together with Its Switching Elements.

In Fig. 1, a typical winding is shown, idealized, on the poles of phase a which is connected to voltage supplies V_{C1} and V_{C2} through a switch (transistor) and diode. It can be noted that since pairs of poles are connected in series, the machine is, in effect, a four phase machine. When the switch T_a is closed, current builds up in the winding of phase a due to the supply voltage V_{C1}. When the switch is opened current flows through the diode D_a since the winding is inductive and voltage $-V_{C2}$ is impressed on the winding. Since the voltage is now the reverse polarity, the current decreases under this condition. The current can be regulated at any desired value by modulating (switching) between these two switching patterns. A third condition clearly exists when the current i_a reaches zero. In this case the current in the winding is zero and the voltage across the winding is determined from the time rate of change of flux linkages due to currents flowing in the remaining three windings.

Pulses of current are supplied to each phase in the sequence a, b, c, d and, for motor operation, each pulse of current causes the most adjacent rotor pole to move towards alignment with the energized stator poles. It can be seen that the rotor steps around the stator in a direction opposite to the sequence of stator pole excitation. The initiation and extinction of current pules are made to occur at specific rotor angles. Motor action is obtained when the current pulse occurs as the inductance is increasing while generation occurs if the current pulse is impressed as the inductance of the winding is decreasing.

A more detailed circuit schematic of the power circuit is shown in Fig. 2. It can be noted that the current in each of the phases is unidirectional, so that only four transistors and six diodes are used to control the current in the four phases. The circuit uses a center tapped dc bus arrangement to feed back energy to the supply when the rotor and stator poles of the phases are aligned and thereby avoid undesirable negative torque components. Other connections are possible which produce the same function but generally with the addition of extra switches, extra losses or extra windings in the machine[10]. Each switching device is equipped with an RC snubber which serves to lessen the switching stresses on the device.

3 MAGNETIC CIRCUIT FORMULATION

Figure 3 shows a magnetic equivalent circuit of the 8/6 pole machine. In general, each stator pole can be considered as having two reluctances, $\mathcal{R}_p$, and $\mathcal{R}_g$ due to the reluctance of the pole body, and gap respectively. In addition, each section of the stator core has been assigned a reluctance $\mathcal{R}_c$. The rotor poles are also represented by pole body and slot reluctances.

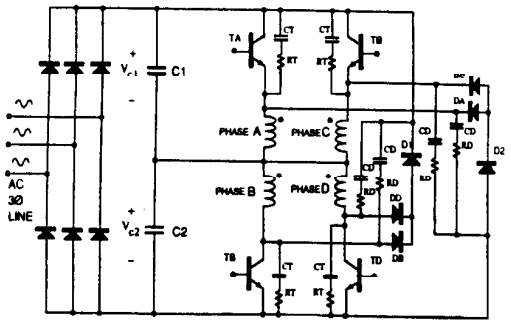

Figure 2: Four Phase SR Motor Showing Converter Circuit Details.

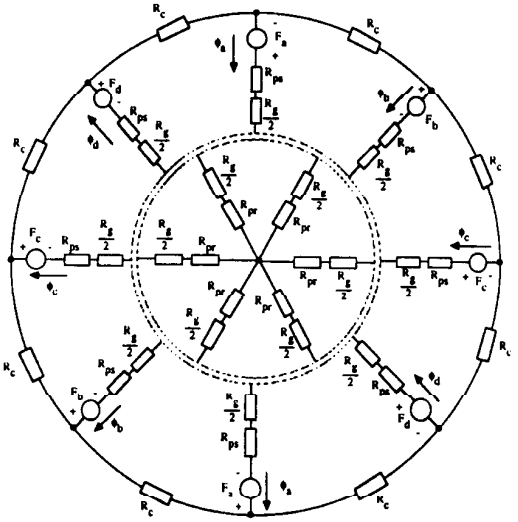

Figure 3: Magnetic Equivalent Circuit of 8 Pole Stator / 6 Pole Rotor Switched Reluctance Motor.

In Fig. 4 the effect of the 6 pole rotor on the air gap flux has been modelled by eight equivalent reluctances, one per stator pole. The stator pole body reluctance and associated MMF has been subdivided into two portions to more accurately represent the actual case in which an infinite number of subdivisions would be necessary. A slot body leakage $\mathcal{R}_{sl}$ has been introduced to represent the flux which crosses the slot and thereby links two coils. The pole reluctance near the pole tip, $\mathcal{R}_{pt}$, is assumed to be saturable while the reluctance at the base of the pole $\mathcal{R}_{pb}$ is assumed to remain constant. It should be noted that this assumption is not strictly correct since the flux density in the pole increases approximately uniformly over the pole so that both $\mathcal{R}_{pb}$ remains roughly equal to $\mathcal{R}_{pt}$. However, the flux circulating in the mutual coupling path - defined by the loop around $\mathcal{R}_{pb}$, $\mathcal{R}_{sl}$, the pole body reluctance of the adjacent pole $\mathcal{R}_{pb}$ and $\mathcal{R}_c$ - is not greatly affected by this assumption because $\mathcal{R}_{sl} \gg \mathcal{R}_{pb}$. Since the rotor poles do not have discrete windings, the rotor body is nearly an equipotential so that the rotor pole reluctance has been simply lumped with the reluctance of the stator pole tip. It is assumed, in effect, that the flux entering one of the rotor poles results from only one of the stator poles. The possibility of flux entering one of the rotor poles from two or more stator poles is therefore neglected. With this assumption the gap reluctances can be connected in a star configuration, the potential of the star point being the average potential of the rotor. Finally, it should be noted that leakage fluxes (flux which links only one winding) are considered separately and are not included in Fig. 3.

Using the equivalent circuit of Fig. 4 the loop equations for the motor can be written. For example, for phase a, taking paths around loops 1,3,5 and 7

$$(F_a - F_b)/2 = \mathcal{R}_c\phi_1 + \mathcal{R}_{pb}(\phi_1 - \phi_3) + \mathcal{R}_{sl}(\phi_1 - \phi_2) + \mathcal{R}_{pb}(\phi_1 + \phi_7) \quad (1)$$

$$(F_b - F_c)/2 = \mathcal{R}_c\phi_3 + \mathcal{R}_{pb}(\phi_3 - \phi_5) + \mathcal{R}_{sl}(\phi_3 - \phi_4) + \mathcal{R}_{pb}(\phi_3 - \phi_1) \quad (2)$$

$$(F_c - F_d)/2 = \mathcal{R}_c\phi_5 + \mathcal{R}_{pb}(\phi_5 - \phi_7) + \mathcal{R}_{sl}(\phi_5 - \phi_6) + \mathcal{R}_{pb}(\phi_5 - \phi_3) \quad (3)$$

$$(F_d + F_a)/2 = \mathcal{R}_c\phi_7 + \mathcal{R}_{pb}(\phi_7 + \phi_1) + \mathcal{R}_{sl}(\phi_7 - \phi_8) + \mathcal{R}_{pb}(\phi_7 - \phi_5) \quad (4)$$

In addition, for each adjacent set of poles, traversing loops 2,4,6 and 8

$$(F_a - F_b) = \mathcal{R}_{sl}(\phi_2 - \phi_1) + (\mathcal{R}_{ptb} + \mathcal{R}_{gb})(\phi_2 - \phi_4) + (\mathcal{R}_{pta} + \mathcal{R}_{ga})(\phi_2 + \phi_8) \quad (5)$$

$$(F_b - F_c) = \mathcal{R}_{sl}(\phi_4 - \phi_3) + (\mathcal{R}_{ptc} + \mathcal{R}_{gc})(\phi_4 - \phi_6) + (\mathcal{R}_{ptb} + \mathcal{R}_{gb})(\phi_4 - \phi_2) \quad (6)$$

$$(F_c - F_d) = \mathcal{R}_{sl}(\phi_6 - \phi_5) + (\mathcal{R}_{ktd} + \mathcal{R}_{gd})(\phi_6 - \phi_8) + (\mathcal{R}_{ptc} + \mathcal{R}_{gc})(\phi_6 - \phi_4) \quad (7)$$

$$(F_d + F_a) = \mathcal{R}_{sl}(\phi_8 - \phi_7) + (\mathcal{R}_{pta} + \mathcal{R}_{ga})(\phi_8 + \phi_2) + (\mathcal{R}_{ptd} + \mathcal{R}_{gd})(\phi_8 - \phi_6) \quad (8)$$

In these equations the quantities $\mathcal{R}_{pta}, \mathcal{R}_{ptb}$.. are assumed to be functions of flux in the poles while $\mathcal{R}_{ga}$, $\mathcal{R}_{gb}$ .. are considered to be functions of the rotor position θ_r. The parameters $\mathcal{R}_{pb}, \mathcal{R}_c$ and $\mathcal{R}_{sl}$ are assumed to be constant.

Upon adding these eight equations the following result can be obtained

$$2F_a = \phi_1(\mathcal{R}_c + 2\mathcal{R}_{pb}) + \phi_2(2\mathcal{R}_{pta} + \mathcal{R}_{ga}) + \phi_3\mathcal{R}_c + \phi_5\mathcal{R}_c + \phi_7(2\mathcal{R}_{pb} + \mathcal{R}_c) + \phi_8(2\mathcal{R}_{pta} + 2\mathcal{R}_{ga}) \quad (9)$$

If Eqs. 1 and 5 are multiplied by -1 and the resulting eight equations added

$$2F_b = -\phi_1(\mathcal{R}_{pb} + 2\mathcal{R}_c) - \phi_2(2\mathcal{R}_{ptb} + \mathcal{R}_{gb}) + \phi_3(\mathcal{R}_{pb} + \mathcal{R}_c) + \phi_4(2\mathcal{R}_{ptb} + \mathcal{R}_{gb}) + \phi_5\mathcal{R}_c + \phi_7\mathcal{R}_c \quad (10)$$

If Eqs. 1,2, 5 and 6 are multiplied by -1 another expression can be obtained involving only the MMF F_c. Finally, if Eqs. 1-3 and 5-7 are multiplied by -1 an expression involving F_d is obtained.

It is useful to express these equations in terms of the fluxes in the base of the pole and in the pole tip. The equations relating ϕ_{ab} ϕ_{at},... to the fluxes ϕ_1, ϕ_2,... are,

$$\phi_1 + \phi_7 = \phi_{ab} \quad (11)$$

$$\phi_3 - \phi_1 = \phi_{bb} \quad (12)$$

$$\phi_5 - \phi_3 = \phi_{cb} \quad (13)$$

$$\phi_7 - \phi_5 = \phi_{db} \quad (14)$$

$$\phi_2 + \phi_8 = \phi_{at} \quad (15)$$

$$\phi_4 - \phi_2 = \phi_{bt} \quad (16)$$

$$\phi_6 - \phi_4 = \phi_{ct} \quad (17)$$

$$\phi_8 - \phi_6 = \phi_{dt} \quad (18)$$

In matrix form Eqs. 1-8 become,

$$\begin{bmatrix} F_a \\ F_b \\ F_c \\ F_d \end{bmatrix} = \begin{bmatrix} \mathcal{R}_{pta} + \mathcal{R}_{ga} & 0 & 0 & 0 \\ 0 & \mathcal{R}_{ptb} + \mathcal{R}_{gb} & 0 & 0 \\ 0 & 0 & \mathcal{R}_{ptc} + \mathcal{R}_{gc} & 0 \\ 0 & 0 & 0 & \mathcal{R}_{ptd} + \mathcal{R}_{gd} \end{bmatrix} \cdot \begin{bmatrix} \phi_{at} \\ \phi_{bt} \\ \phi_{ct} \\ \phi_{dt} \end{bmatrix} + \begin{bmatrix} \mathcal{R}_{pb} + \mathcal{R}_c & -\mathcal{R}_c/2 & 0 & \mathcal{R}_c \\ -\mathcal{R}_c & \mathcal{R}_{pb} + \mathcal{R}_c & -\mathcal{R}_c & 0 \\ 0 & -\mathcal{R}_c & \mathcal{R}_{pb} + \mathcal{R}_c & -\mathcal{R}_c \\ \mathcal{R}_c & 0 & -\mathcal{R}_c & \mathcal{R}_{pb} + \mathcal{R}_c \end{bmatrix} \cdot \begin{bmatrix} \phi_{ab} \\ \phi_{bb} \\ \phi_{cb} \\ \phi_{db} \end{bmatrix} \quad (19)$$

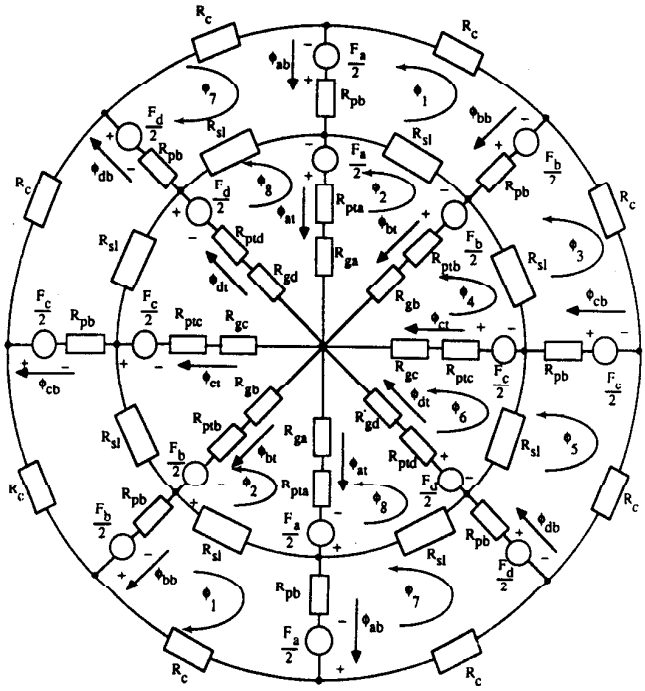

Figure 4: Simplified Magnetic Equivalent Circuit of 4 phase Switched Reluctance Motor.

It is interesting to note that when the pole tip and pole base fluxes are used as variables, the off-diagonal terms of the reluctance matrix, (resulting in mutual coupling) are independent of the slot reluctance $\mathcal{R}_{sl}$.

If the leakage is assumed to be confined to the pole tips, the reluctance of the leakage path is defined by, for example,

$$F_a/2 = (\mathcal{R}_{pta} + \mathcal{R}_\ell)\phi_{al} + 2\mathcal{R}_{pta}\phi_{at} \tag{20}$$

However, the reluctance of the leakage path through air $\mathcal{R}_\ell$ is much greater than than the portion of the path through the pole tip $\mathcal{R}_{pta}$, the leakage reluctances are essentially linear and defined by,

$$\begin{bmatrix} F_a \\ F_b \\ F_c \\ F_d \end{bmatrix} = \begin{bmatrix} 2\mathcal{R}_\ell & 0 & 0 & 0 \\ 0 & 2\mathcal{R}_\ell & 0 & 0 \\ 0 & 0 & 2\mathcal{R}_\ell & 0 \\ 0 & 0 & 0 & 2\mathcal{R}_\ell \end{bmatrix} \cdot \begin{bmatrix} \phi_{al} \\ \phi_{bl} \\ \phi_{cl} \\ \phi_{dl} \end{bmatrix} \tag{21}$$

The total flux linking the pole is finally

$$\phi_a = \phi_{al} + \phi_{at} \tag{22}$$

and to forth for ϕ_b, ϕ_c, and ϕ_d.

The flux linkages of a particular stator phase (two series connected stator poles) due to the current in any phase (impressed on any pair of poles) can now be readily calculated. The assumption that the saturation of the iron takes place in the half of the stator pole near the tip makes the solution of the circuit particularly simple. In terms of inductances the solution for the stator magnetic equivalent circuit of Fig. 3 takes the form

$$\begin{bmatrix} i_a \\ i_b \\ i_c \\ i_d \end{bmatrix} = \begin{bmatrix} 1/L_{ptga} & 0 & 0 & 0 \\ 0 & 1/L_{ptgb} & 0 & 0 \\ 0 & 0 & 1/L_{ptgc} & 0 \\ 0 & 0 & 0 & 1/L_{ptgd} \end{bmatrix} \cdot \begin{bmatrix} \lambda_{at} \\ \lambda_{bt} \\ \lambda_{ct} \\ \lambda_{dt} \end{bmatrix}$$
$$+ \begin{bmatrix} 1/L_{pbc} & -1/L_{m1} & -1/L_{m2} & 1/L_{m1} \\ -1/L_{m1} & 1/L_{pbc} & -1/L_{m1} & -1/L_{m2} \\ -1/L_{m2} & -1/L_{m1} & 1/L_{pbc} & -1/L_{m1} \\ 1/L_{m1} & -1/L_{m2} & -1/L_{m1} & 1/L_{pbc} \end{bmatrix} \cdot \begin{bmatrix} \lambda_{ab} \\ \lambda_{bb} \\ \lambda_{cb} \\ \lambda_{db} \end{bmatrix} \tag{23}$$

In this equation, $\lambda_{ab} = 2N\phi_{ab}$ and $i_a = F_a/N$ and so forth.

The inductances L_{ptga} ... etc. represent the series equivalent of the pole tip and air gap reluctances and are thus a function of both the flux linkage λ_{at} ... etc. and the rotational angle θ_r. For example, L_{ptga} is, for example, expressed,

$$L_{ptga} = \frac{N^2}{\mathcal{R}_{pta}(\phi_{pta}) + \mathcal{R}_{ga}(\theta_r)} \tag{24}$$

where the functional dependence of the reluctances is explicitly shown.

It should be noted that the second inductance matrix contains only constants which makes the solution of the differential equations relatively straightforward. Also, it is important to observe the introduction of an additional inductance L_{m2}. This extra inductance arises due to the presence of the actual six pole rotor structure which has been replaced in this analysis by an equivalent eight pole rotor. While this inductance is small, it has been included in the solution since tests have indicated the importance of this term. The presence of this inductance is not predicted by the simplified analysis of Fig. 4. In practice, the inductances L_{m1} and L_{m2} vary somewhat with rotor position. However, if the average value of these inductances are used which apply during the instant during which the mutual coupling is effective, (i.e. when i_a and i_b overlap for example) the solution can be shown to be not much affected. affected.

4 DETERMINATION OF EQUIVALENT CIRCUIT PARAMETERS

Since the actual paths encountered by the flux in a SR motor is difficult to predict with simple magnetic circuits, the inductances described by Eq. 9 must be determined either through test or by means of a finite element analysis. Test results typically yield a series of flux-linkage versus current curves with one phase excited for various rotor angles. In this case the flux linkage represents the total flux linking the winding and the current represents the total current required to magnetize the base of the pole and stator core as well as the pole tips and the gap. The useful portion of the flux must therefore be estimated by subtracting from these curves a leakage flux component obtained either by finite elements [4] or other conventional methods [11]. In addition, the effect of magnetizing the reluctance of the pole base and core should be eliminated from the measured flux versus current relationships. In this case, since the permeance of the path decreases, the flux must be increased for a given current. In practice, these two effects nearly cancel and since the overall effect is small at any rate, the measured flux linkage versus current curves can be use to represent the flux linkage of the pole tip versus the current required to magnetize the pole tip. The mutual coupling due to slot body leakage can also be obtained by test since the flux linking phase b due to a current in phase a can be readily obtained. If the effects of the core, pole body and the leakage path are assumed to cancel, the individual components of this inductance corresponding to $\mathcal{R}_{sl}$, $\mathcal{R}_{pb}$ and $\mathcal{R}_c$ would not be required for simulation purposes but could be estimated, if desired, by magnetic equivalent circuits, the use of search coils or by finite element analysis.

5 SIMULATION EQUATIONS

The equations which describe transient behavior of the switched reluctance motor can now be established. The equations for the total flux linking the individual phase windings are

$$\lambda_a = \int_0^t [v_a - r_a i_a] \cdot dt \tag{25}$$

and so forth for phases b, c and d. If L_ℓ denotes the total leakage inductance of each phase the flux linking the pole tip can be written as

$$\lambda_{at} = \lambda_a - (L_\ell - L_{pb} - 2L_c)i_a \tag{26}$$

or simply

$$\lambda_{at} = \lambda_a - L'_\ell i_a \tag{27}$$

and so forth for λ_{bt}, λ_{ct} and λ_{dt}.

It is useful to let i_{a1} equal the current flowing in phase a due to the magnetization of the rotor pole and stator pole tip, while i_{a2} denotes the current flow resulting from magnetization of the core and slot body leakage path. Rather than solve for the non-linear inductance L_{ptga} the solution for i_{a1} is more conveniently obtained directly from the λ versus i characteristics. Hence,

$$i_{a1} = f(\lambda_{at}, \theta_r) \tag{28}$$

and so forth for i_{b1}, i_{c1} and i_{d1}. The solution for i_{a2} is linear and obtained the second term in Eq. 9.

The voltage across an individual phase is obtained by logic equations which govern when the respective switches close. For example, for phase a

$$v_a = v_{C1} \text{ if } \theta_{on} \le \theta_r \le \theta_{off} \tag{29}$$

$$v_a = -v_{C2} - v_{D1} \text{ if } \theta_r > \theta_{off} \tag{30}$$

where

$$v_{D1} = 0 \text{ if } i_a > 0 \tag{31}$$

and

$$v_{D1} = \frac{1}{C_D}\int i_a \cdot dt + i_a r_D \text{ if } i_a < 0 \tag{32}$$

where v_{D1} equals the voltage across the snubber circuit of diode D_1. Similar equations apply for phases b, c and d.

The torque can be calculated by conventional means, that is

$$T_e = -\frac{\partial W_f}{\partial \theta_r}|_{\lambda_a,\lambda_b,..=\text{const.}} \tag{33}$$

where W_f is the energy stored in the field at any instant, i.e.

$$W_f = \int_0^{\lambda_a,\lambda_b,\lambda_c,\lambda_d} i_a \cdot d\lambda_a + i_b \cdot d\lambda_b + i_c \cdot d\lambda_c + i_d \cdot d\lambda_d \tag{34}$$

A complete block diagram of the simulation is shown in Fig. 5. Of particular interest is the computation block used to develop the torque, Eq. 33. Since the ACSL program allows for Fortran subroutines, it has been found convenient to use the spline fit package available as part of the IMSL subroutine library. The flux linkage versus current curves are input as a series of points and a spline fit program produces a quadratic fit between each series of points. The spline fit assure not only continuity of the function between each set of points but also a continuous derivative. Another spline program is then used to perform the integration to obtain the field energy, Eq. 34, and a third spline program is invoked to perform the derivative to obtain the torque, Eq. 33. The entire process can therefore be accomplished with only three calls to IMSL subroutines.

6 SIMULATION RESULTS AND COMPARISON WITH TEST

Using the equations of the previous section a complete simulation of a switched reluctance motor driven from a converter supply has been written in the digital computer code ACSL (Advanced Computer Simulation Language). The system chosen for study was an 10 HP, 1500 RPM SR motor drive manufactured by Oulton. A summary of parameters of the motor and converter used for the simulation is given in Table 1. A plot of the measured flux linkage versus current curves for this machine are shown in Fig. 6.

Figures 7 and 8 show both simulated and measured flux linkage versus current loci for operation at 1000 RPM. The machine is operating at no-load so as to enhance the second order effects which are usually neglected. In Figs. 9 and 10 are shown the current and voltage versus time curves for both the simulated motor and the actual SR motor drive. Excellent agreement between simulated and test results are apparent. For completeness a trace of the calculated electromagnetic torque of the motor is shown in Fig. 11. The corresponding torque of the actual drive was not measured due to present difficulty in instrumentation.

Of particular interest is the oscillations which occur across each phase when the feedback diode stops conduction. A more detailed plot showing the voltage across all four of the phases is shown in Fig. 12. The influence of turn off of adjacent phases can be observed by additional oscillations during the normal off period of the phase. These additional oscillations are caused by the mutual coupling between phases which is normally neglected. Also it has been observed that the frequency and damping of the voltage ringing across the phases during turn off are also strongly dependent on this mutual coupling effect. Hence, the mutual coupling is an important parameter if close correlation of measured and test results are to be expected.

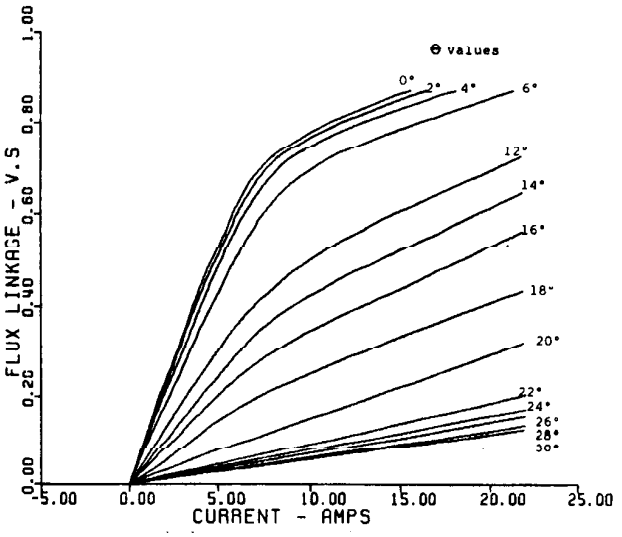

Figure 6: Flux Linkage Curves Versus Current and Rotational Angle θ_r for 10 HP Oulton Machine.

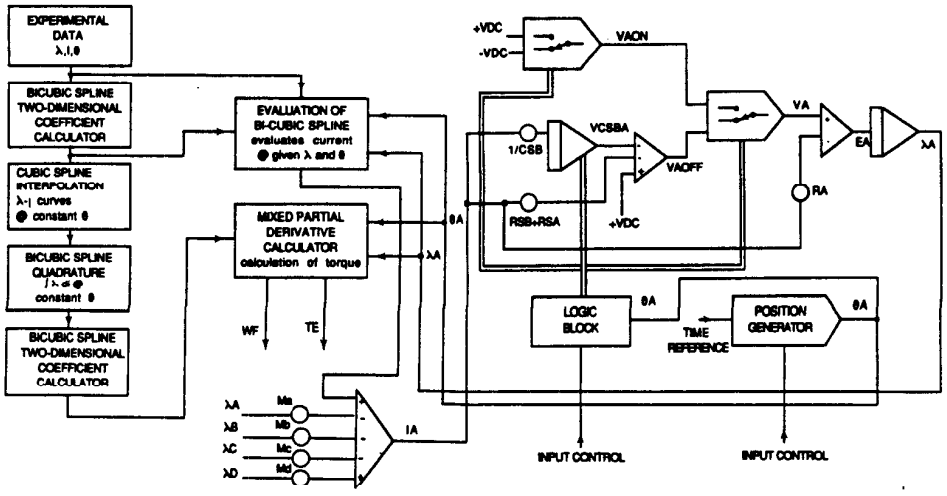

Figure 5: Simulation Diagram for 4 Phase Switched Reluctance Motor Including the Effects of Mutual Coupling. Simulation of Only One of Four Phases is Shown.

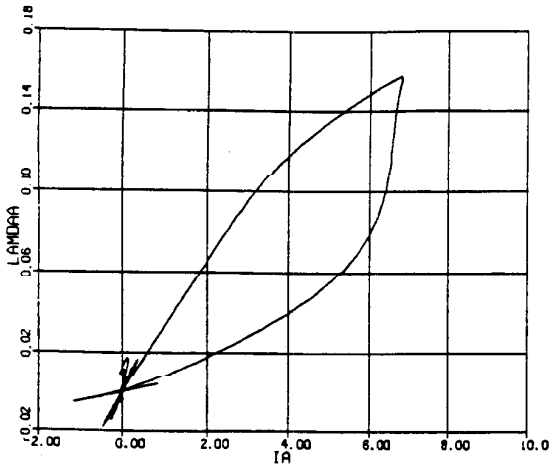

Figure 7: λ vs. i Locus for Simulated 10 HP Oulton Motor Drive. No-load Operation at 1000 RPM.

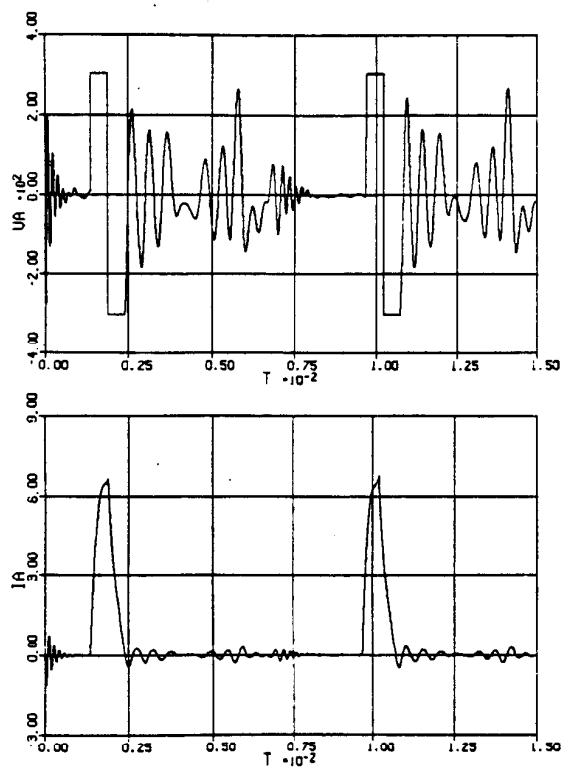

Figure 9: (a) Phase Voltage and (b) Phase Current of 10 HP SR Motor Drive. Simulated Results.

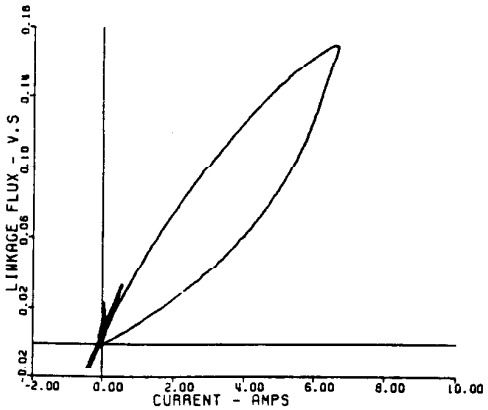

Figure 8: Measured λ vs. i Locus for 10 HP Oulton Motor Drive. No-load Operation at 1000 RPM.

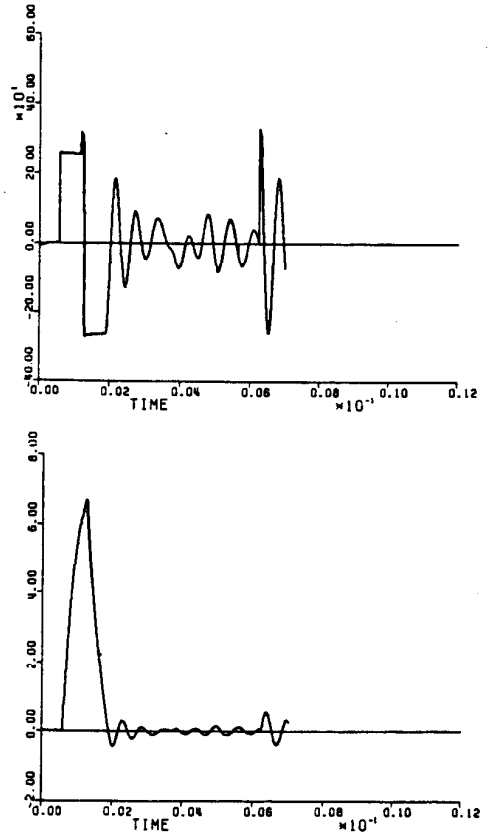

Figure 10: (a) Phase Voltage and (b) Phase Current of 10 HP SR Motor Drive. Measured Results from Test.

Perhaps more significant effects of the presence of mutual coupling are shown by the traces in Fig. 13. This figure shows the four phase currents during a more heavily loaded condition of 25% of rated load at 1000 RPM. It can be noted that an overlap condition begins to appear in which two adjacent phases conduct simultaneously. The current in the phase begins to develop a "tail" which increases losses and could even cause negative torque to occur should the tail persist for a long enough time. This change in slope of the off-going current is caused by voltage induced due to the negative mutual coupling between adjacent phases, *a* and *b* for example, which tends to oppose the voltage V_{C2}.

In Fig. 13 is also shown the electromagnetic torque produced only by the phase *a* current is plotted for the same operating condition. In addition to the usual positive going pulse of torque, a negative component can be noted occurring at the instant that phase c conducts. This negative torque again results from negative mutual coupling, this time between phases *a* and *c*. In this case, a voltage is induced in phase *a* which tends to produce current flow around the path defined by the phase *a* coil, the capacitor *C2* and the feedback diodes *D2* and *DA* in Fig. 2. It is interesting to note that since the coupling between phases *a* and *d* is positive rather than negative, a similar negative torque pulse does not occur when phase *d* begins to conduct.

It is clear that current tailing and negative torque components must be minimized if the motor is to operate at high efficiency. It is also apparent that these effects, while qualitative at this stage, can only be examined with proper attention to the mutual coupling between phases. Work on modelling of mutual coupling effects is continuing at the University of Wisconsin.

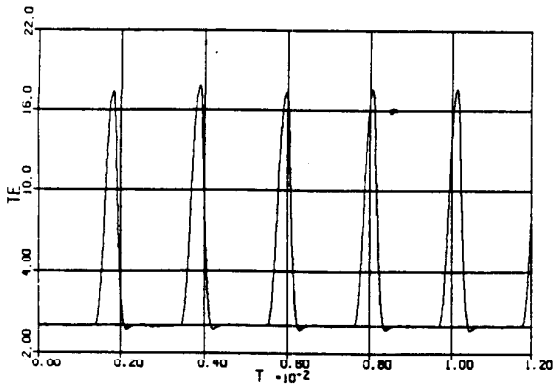

Figure 11: Electromagnetic Torque Correponding to Figs. 7 and 8.

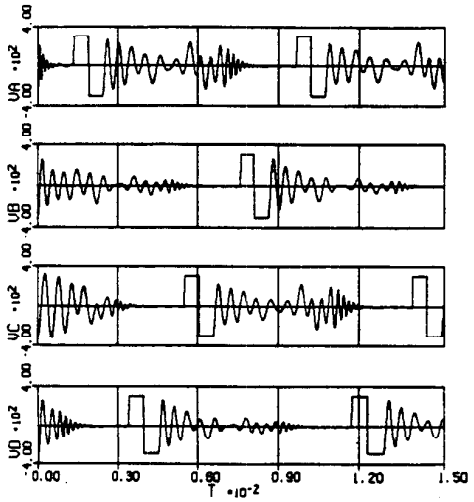

Figure 12: The Four Phase Voltages for the Condition of Figs. 7,8 and 10.

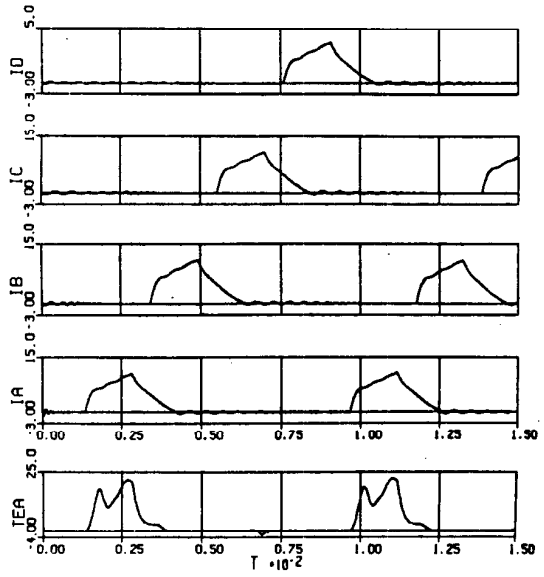

Figure 13: Four Phase Currents and Electromagnetic Torque Produced by Phase *a* for the Loaded Condition of 0.25 pu and 1000 RPM. Note the Current Tail in Phase *a* after Conduction of Phase *b* and the Negative Torque Pulse Occuring When Phase *c* Conducts.

7 CONCLUSIONS

This paper has introduced a new coupled circuit model for a switched reluctance motor drive. The model includes the effect of mutual coupling between phases which has been neglected in prior models of the machine. The mutual coupling has been shown to have an important effect on the open circuit voltage waveform across each phase winding. The mutual inductance also affects the turn off time of the phase current resulting in reduced torque and added losses. Finally, mutual inductance can also contribute to unwanted conduction during the nominal "off" period of a phase winding, thereby also contributing extra losses together with undesirable torque components.

8 ACKNOWLEDGMENT

The authors wish to acknowledge the Whirlpool Corp. for support of this project.

9 REFERENCES

1. P.J. Lawrenson, J.M. Stephenson, P.T. Blenkinsop, J. Corda and N.N. Fulton, *Variable-Speed Switched Reluctance Motors*, Proc. IEE, Vol. 127, Pt. B, No. 4, July 1980, pp. 253-265.

2. T.J.E. Miller and T.M. Jahns, *A Current-Controlled Switched-Reluctance Drive for FHP Applications*, Proceedings of the Conference on Applied Motion Control (CAMC) Minneapolis, MN, June 1986, pp. 109-117.

3. W.F. Ray, R.M. Davis, P.J. Lawrenson, J.M. Stephenson, N.N. Fulton and R.J. Blake, *Switched Reluctance Motor Drives for Rail Traction: A Second View*, IEE Proceedings, Vol. 131, Pt. B, no. 5, September 1984, pp. 220-225.

4. G.E. Dawson, A.R. Eastham, J. Mizia, *Switched Reluctance Motor Torque Characteristics: Finite Element Analysis and Test Results*, 1986 IEEE/IAS Annual Meeting Conference Record, pp. 864- 869.

5. T.J.E. Miller, *Converter Volt-Ampere Requirements of the Switched Reluctance Motor Drive*, 1984 IEEE/IAS Annual Meeting Conference Record, pp. 813-819.

6. M. Illic'-Spong, T.J.E. Miller, S.R. MacMinn and J.S. Thorp, *Instantaneous Torque Control of Electric Motor Drives*", Proc. IEEE Power Electronics Specialist's Conference. Toulouse France, June 1985 pp. 42-48.

7. J.M. Stephenson and J. Corda, *Computation of Torque and Current in Doubly Salient Reluctance Motors from Non-Linear Magnetization Data*, Proc. IEE, Vol. 126, No. 5 May 1979, pp. 393- 396.

8. G. Singh, *Mathematical Modelling of Step-Motor*, Proceedings of the Incremental Motion Control System Devices Conference, Champaign IL, pp. 59- 148.

9. I.E.D. Pickup an d D. Tipping, *Method for Predicting the Dynamic Response of a Variable Reluctance Stepping Motor*," Proc. IEE, Vol. 120, 1973, pp. 757-765.

10. J.T. Bass, T.J.E. Miller, R.L. Steigerwald, *Development of a Unipolar Converter for Variable Reluctance Motor Drives* 1985 IEEE/IAS Annual Meeting Conference Record. pp. 1062-1068.

11. M. Liwshitz-Garik and C.C. Whipple, *Electric Machinery*, (book) D. Van Nostrand Co., Inc, New York, 1946.

Pole Tip and Gap Rcluctance: L_{ptga}	See Fig. 7
Mutual Coupling Between Adjacent Phases: L_{m1}	150 mH.
Mutual Coupling Between Non-Adjacent Phases: L_{m2}	50 mH.
Phase Resistance: r_a	0.32 Ω
Diode Snubber Resistance: r_D	33 Ω
Diode Snubber Capacitance: C_D	0.001 μf
Filter Capacitance: C_1,C_2	1360 μf

Table 1
Parameters of 10 HP Oulton Switched Reluctance Motor.